International Journal of Modern Chemistry, 2018, 10(2): 268-289

Modern Scientific Press

International Journal of Modern Chemistry **ISSN: 2165-0128**

Journal homepage: www.ModernScientificPress.com/Journals/IJMChem.aspx *Florida, USA*

Article

Adsorption Activity of Graphene oxide /Aluminum-based MOF for Removal of Congo Red Azodye

Awad. I. Ahmed, W.S. Abo El-Yazeed, H.Z. El-Shenawy, B.N. Mansour*

Chemistry Department, Faculty of Science, Mansoura University, Mansoura, Egypt

*Author to whom correspondence should be addressed; E-Mail: basmanasermansour1992@gmail.com

Article history: Received 23 August 2018, Revised 30 September 2018, Accepted 15 October 2018, Published 22 October 2018.

Abstract: Congo Red (CR) azodye adsorption from aquatic solution using MIL-101 Al and graphene oxide based on MIL-101(Al) by different weight percentage was studied. The hydrothermal method applied for preparation of MIL-101 and different wt% GO/MIL-101 catalysts. The prepared catalysts were described by XRD, FT-IR, and TEM. Batch experiments were studied for adsorption kinetics and isotherms. Experimental data obtained indicated that the process of adsorption was extremely dependent on contact time, the concentration of dye and adsorbent dosage. The prepared nanocataysts (1, 3 and 5 wt% GO/MIL-101(Al) samples) indicated preferred outcomes in adsorption over pure MIL-101 until 10 wt% GO/MIL-101(Al). Adsorption equilibrium of 1 wt% GO/MIL-101(Al) was reached equilibrium within 2 hrs, and the amount of adsorption achieved up to 96%. The dynamic adsorption set up by a pseudo-second-order kinetic model, and Langmuir isotherm model was best model applicable for calculating the equilibrium parameters.

Keywords: Graphene oxide, MIL-101 (Al), adsorption, Congo red.

1. Introduction

Over the last at least three decades, as a result of increasing water pollution the green chemistry was

interested in water purification. The important rule in green chemistry fundamental was preparation solid nanocatalysts that used in treating drinking water and these nanocatalysts could be reused a lot of times. These nanocatalysts have discovered an extensive number of uses in numerous fields, such as catalysis, separation, adsorption, and purification [1,2]. MOFs a new kind of porous solid nanocatalysts, appeared almost two hundred years ago and have since immediately formed into a productive research field [3-7]. MOFs catalysts were linked with metal particles and nature ligands have taken a great concern taking into account the high surface-active sites and the species of pore structures [8-10]. MOFs properties noticed diverse from those of each composite [10]. MOFs had a lot of advantages which were the appropriate structure, elasticity, presence of a lot of pores with ordered crystalline pores and different types of effective properties can be important, so that, appearance of new chemical and physical properties that are not founded by each composite [11-13]. Graphene oxide sheets were prepared by oxidizing of graphite powder. Structure of hexagonal carbon atoms generates enough dispersion force help in increasing adsorption efficiency [14]. In addition, GO consists of oxygen functionalities (carboxyl group, the hydroxyl group, epoxy group) on its multilayer morphology [15,16]. Therefore, GO had great potential for the arrangement of composite substances by virtue of the unique structure of layers and surface qualities. Also, GO totally dispersed well in water or in some other polar solvents due to its hydrophilic properties [17].

Artificial organic dyes are major types of compounds and are often present in the environment (as pollutants in wastewater), due to their wide manufacturing applications. The color of the water is the first thing to be known in wastewater and the existence of very small amounts of organic dyes in aqueous solutions is extremely obvious and unfavorable. Lack of attention to this problem, the greatest environmental attention with dyes was their absorption and reflection of sunlight penetrating the water, which caused the growth of bacteria [18]. A lot of dyes can be harmful to aquatic life and also to human beings due to its toxic [19]. So, getting rid of such synthetic colored dyes from aqueous solutions is of significant environmental and technical importance. There are a lot of methods tried to get rid of pollutants from textile, plastics, paper effluents, pulp, and dyestuffs, however, have been accepted by these manufactures [20-24]. Many various techniques including nanofiltration, cloud point extraction, ozonation, oxidation processes and coagulation have been used to get rid of colored dyes from wastewater [25-28]. Adsorption technique was the most popular method to get rid of non-biodegradable pollutants (including dyes) from wastewater due to its simplicity, it is inexpensive, the availability of a wide range of adsorbents, easy operation and the possibility of re-using [29-33].]. As a result of increasing water pollution, green chemistry was interested in water purification. The important rule in green chemistry fundamental was preparation solid nanocatalysts that used in treating drinking water and these nanocatalysts could be reused a lot of times. In this paper, we studied the removal of congo red dye using adsorption technique by MIL-

101 and different wt% GO/MIL-101 as nano-adsorbents. Congo red (CR) dye was a secondary diazo dye (anionic dye). It is used for the coloring cotton and as a pH indicator and it is sensitivity to light and acids [34]. This dye was known to be harmful it caused human carcinogen. Treatment of wastewater consists of azo dyes was difficult to decompose because they were not much sensitive to biological degradation [35].

MIL-101(Al) and GO loaded on MIL-101(Al) were favorable nanocatalyst adsorbents for disposal from congo red dye from wastewater due to their high surface area and the big size of pores. The pores presence on these adsorbent surfaces could adsorbate a large amount of congo red dye solution. MIL adsorbents contain polar and polarizable bonds, and can even open coordination active sites on metal. Thus, electrostatic or coordinative properties can control increase or decrease the adsorptive removal of the dye due to its structure [3,36].

Up to now, a lot of nanocataysts of MIL/GO and their applications have been mentioned. Bandosz's group has prepared MOF-5/GO, MOF-199/GO, and MIL-100(Fe)/GO, which were used in ammonia adsorption [37-39]. Zhang et al. [40] synthesized MIL-53(Fe)/rGO for the photodegradation of methylene blue. Zhou et al. [41] prepared MIL-101(Cr)/GO and applied in adsorbing acetone vapor. In this paper, we studied the removal of congo red dye using adsorption technique by MIL-101 and different wt%GO/MIL-101 as nano-adsorbents.

2. Materials and Methods

2.1. Materials

For preparation MIL-101(Al) we used Aluminum chloride ($AlCl_3$, 99%), terephthalic acid (HO_2C-C_6H_4-CO_2H, 99 %) N,N-dimethylformamide ($(CH_3)_2NCHO$, >99.9%) and Sigma Aldrich Methanol. For synthesis Graphene oxide, we used Graphite powder (99.9995%) from alpha, potassium permanganate ($KMnO_4$), 30 % hydrogen peroxide (H_2O_2) from ADWIC, sodium nitrate ($NaNO_3$) and concentrated sulfuric acid (H_2SO_4). Congo Red dye from Sigma Aldrich.

2.2. Synthesis of Materials

MIL-101(Al) was prepared by means of a solvothermal method using N, N-dimethylformamide (DMF) ($(CH_3)_2NCHO$, > 99.9%, 25 ml) as solvent [42]. Starting reactants are Aluminum chloride ($AlCl_3$, 99%, 2.5 mmole, 0.3325 g), terephthalic acid (HO_2C-C_6H_4-CO_2H, 99 %, 5 mmole, 0.8305g). The reactants were put in an autoclave in an oven for 72 hrs at 130^o C in an oven under fixed conditions. The resulting white powder was washed twice by N, N- dimethylformamide (DMF). Then to get rid of organic species restricted within the pores, the substance was activated in boiling methanol 4 hrs and dried at 120 ^{o}C.

GO sheets were prepared according to the modified Hummers and Offeman method from graphite

(99.9995% purity) [43-47]. Get 115 ml of concentrated H_2SO_4, and then put 5g graphite powder and 2.5 g $NaNO_3$ in 2 Liter Beaker, let the mixture stirred vigorously in the ice bath at 0^o C for about 2 hrs using mechanical stirrer, after that 15 g potassium permanganate ($KMnO_4$) was slowly added over about 3 hrs. (Under adjusting temperature to be below 20^o C), and cooling was completed in 2 hrs. The mixture turns to a yellowish green color. Then, take out the mixture from the ice bath and it was permitted to stirrer vigorously overnight at room temperature. As the reaction occurred, the mixture gradually thickened and turns two brown color. 200 ml of dist. H_2O was added slowly to the mixture causing intense effervescence, resulted from the oxidation of $KMnO_4$ accompanied with rising the temperature. The temperature was kept under 98^o C until the end of the effervescence and the color of suspension changed to brown. After 30 min, 700 ml of boiled dist. H_2O was added to the mixture. When the temperature was cooled down to 60^o C, 100 ml of H_2O_2 (30 wt.%) was added to reduce the remaining KMnO4 and the suspension turns bright yellow color. Then the solution washed 3 times with HCl (10%) then with H_2O a lot of times until complete removal of H_2SO_4. The H_2SO_4 remaining tested by using $BaCl_2$ to form a white precipitate of $BaSO_4$. Then dried at 80^o C overnight, finally, we get graphene oxide sheets.

The nanocatalyst GO/MIL-101(Al) was synthesized by using a similar method in preparation of MIL-101 (Al). GO/ MIL-101 (Al) synthesized by solvothermal method. Four percentages of nanocatalyst with different content of GO were synthesized, which were 1, 3, 5 and 10 wt% of the final material percentage weight. Suspension of GO was prepared using DMF as solvent and put in a Teflon-lined autoclave with MIL-101 precursors.

2.3. Characterization Methods

The powder XRD patterns of the prepared adsorbents were registered at the low and high angle using PW 150 (Philips) using Cu Kα radiation source and Ni filter. Fourier transform-infrared (FT-IR) spectra were received in a Thermo- Nicolet spectrometer (ATR-IR Affinity-1, Shimadzu, Japan). Nanocatalyst structures were noticed on a scanning electron microscopy (SEM; JEOL-JSM-6510LV). Transmission electron microscopy (TEM) images and particle size were received using JEOL-JEM-2100 transmission electron microscope.

2.4. Preparation of Congo red (CR) Azodye Solution

A stock solution (1000 mg/L) of congo red (CR) azodye was synthesized in deionized water and solutions used in experiments of wanted CR concentrations were prepared by consecutive dilutions. The concentration of Congo red (CR) azodye solutions used in the experiments calculated from the calibration curve noticed by measuring absorbance of different predetermined concentrations of CR solutions at λ_{max} 497 nm using UV/visible spectrophotometer (Unicom 5625 UV/Vis Spectrophotometer, Perkin Elmer, USA)

[48]., the structure of CR dye in Fig.1.

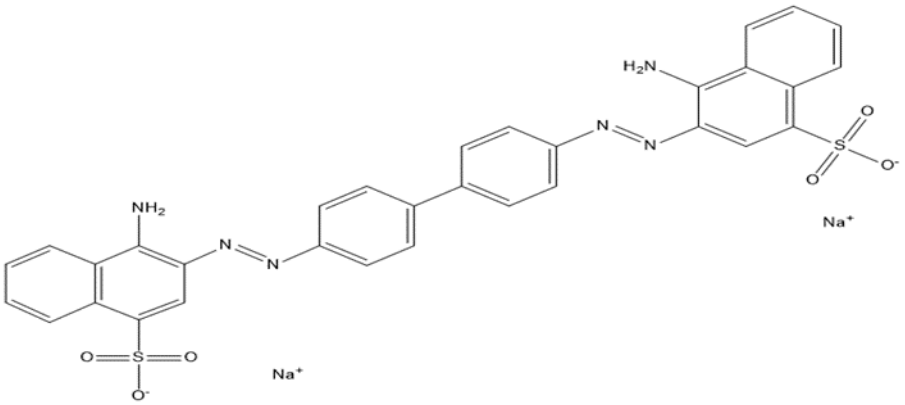

Fig. 1: Congo red dye structure

2.5. Batch Adsorption Experiment

The synthesized samples were applied for getting rid of CR azodye from aqueous solution. For adsorption experiments, different amounts (0.02, 0.03, 0.04, 0.05 and 0.06) of the ultrasonicated prepared sample was weighed in different Pyrex bottles of 100 ml capacity and 50 ml of dye solutions of known concentration (50, 100, 150, 200, 250, 300 and 400ppm) was added. The bottles with their contents were shaken for contact time at room temperature (25^o C) for equilibration [49]. The amount adsorbed was calculated from the difference between the initial and the equilibrium concentrations of Congo Red dye in the aqueous solution then calculate removal percentage based on equation (1).

$$\text{Dye removal \%} = \frac{(C_o - C_e)}{C_o} \times 100 \qquad (1)$$

The amount of Congo red (CR) azodye adsorbed (mg/g) was determined based on a mass balance equation (2) [50]:

$$q_e \text{ (amount of adsorption)} = \frac{(C_o - C_e) \times V}{w} \qquad (2)$$

3. Results and Discussion

3.1. Characterization

The X-ray diffraction patterns of Graphene oxide, and MIL-101(Al) as well as wt% GO/MIL-101(Al), are observed in Fig.2. XRD pattern of MIL-101 displayed diffraction peaks located at 9.0^o, 10.0^o, 15.3^o, 16.9^o, 17.7^o, 18.3^o and 20.9^o, which were compatible with the reported previous studies [51,52],

indicating the successful synthesis of MIL-101. For Graphene oxide, a detach diffraction peak at 10.5° was noticed, interview with layer distance of about 8.4 Å according to Bragg's law. But the special peak of graphene oxide was hidden in wt% GO/MIL-101, for which the low percentage content of Graphene oxide in the species or the high dispersion of Graphene oxide in DMF Based on sonication [53,54]. In wt% GO/MIL-101 composites, the diffraction patterns were noticed that they were similar to that of MIL-101, showing that the crystal structure of MIL-101(Al) has been preserved in composites. In addition to, the peak intensity of wt% GO/MIL-101(Al) nanocatalysts were lower than that of MIL-101, supposing that Graphene oxide prevented the appropriate crystallization of MIL-101 and then resulted in the slight distortion of MOF structure [55-57].

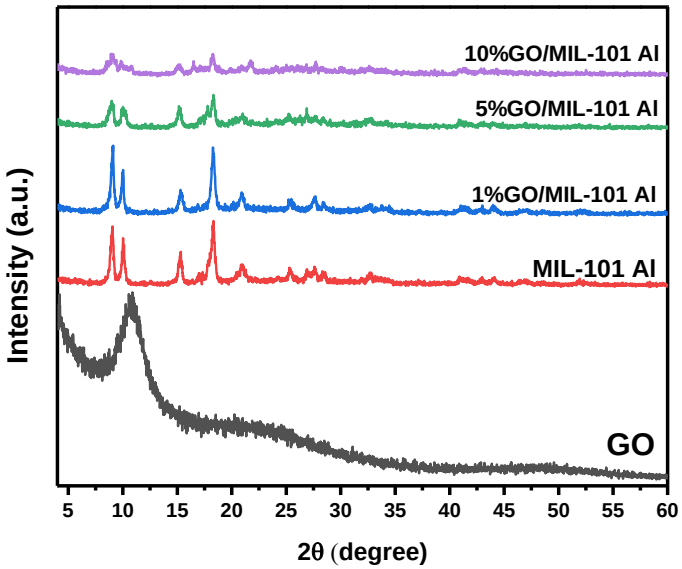

Fig. 2: XRD patterns of GO, parent material MIL-101 and 1,5 and 10 wt% GO/ MIL-101 composites

The FTIR spectrum of GO, MIL-101 and GO/ MIL-101 are drawn in Figure (3). For graphite oxide, the peak at 3448cm^{-1} can be associated with O–H stretching vibrations of adsorbed water molecules and structural OH groups, and the peak at 1651 cm^{-1} can be associated with O-H bending vibrations [58]. The existence of epoxy and carboxyl functional groups can also be revealed at around 1739 cm^{-1}, 1254 cm^{-1} and 1065 cm^{-1}, respectively [59]. At MIL-101, the peak at 3655 and 887 cm^{-1} could be categorized as the hydroxide of the octahedral $AlO_4(OH)_2$ structure [51,52]. Around 3444 cm^{-1}, O–H stretching vibration was appeared indicated presence of free water. Between 1417 and 1677 cm^{-1}, there were asymmetrical stretching vibrations indicated the presence of organic ligands [54]. Otherwise, the vibrations of C=O and C–N due to the increasing of DMF were appeared at 1870 cm^{-1} and 1273 cm^{-1}, respectively. According to MIL-101(Al), wt%GO/MIL-101 nanocatalysts had similar vibration peaks, which was in correspondence with XRD data. The data showed that the higher of Graphene oxide percentage content caused a weakening trend at 1870

cm^{-1} and 1273 cm^{-1}. A conceivable clarification would be that graphene oxide layers helped in Stack prevention of MIL-101, by that way the increasing DMF in nanocatalysts became lowered [60]. Seeing that the MIL-101, the band around 3444 cm^{-1} approximately hidden in the spectrum of wt% GO/MIL- 101, which may be due to the distortion of the structure of MOF framework.

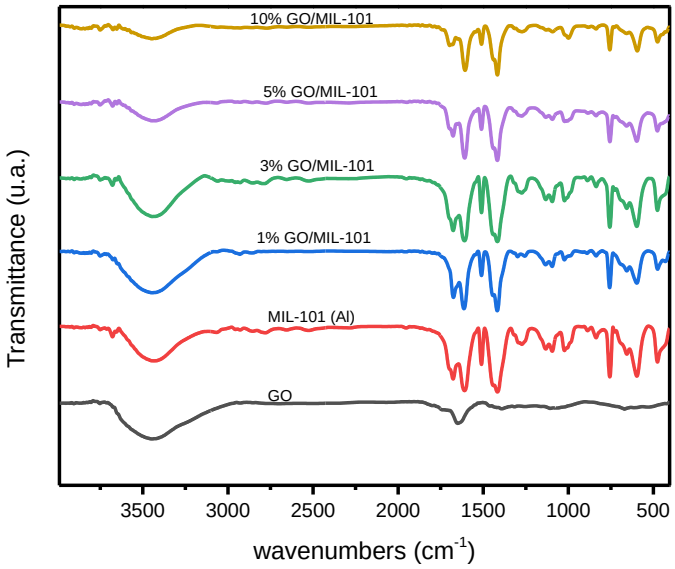

Fig. 3: FTIR spectra of GO, parent material MIL-101(Al) and 1,3,5 and 10 wt% GO/ MIL-101 species

The TEM images of MIL-101 and different wt% GO/MIL-101(Al) species are plotted in Fig. 4. The TEM images of MIL-101 (Al) showed irregular and similar hexagonal nanoparticles with a diameter in a range 200 nm to 400 nm Fig. (4a). Fig. (4b ,4c, 4d) shows the TEM images of 1, 5 and 10wt% GO/MIL-101 respectively, appears as nano-sheets on MIL-101 (Al) crystals with nanosize from 40-80 nm. The image GO entered the pores of MIL-101 (Al) catalysts was not shown as expected, this might be because of the great size of MIL-101 (Al) particles and thickness of the pores which stops the electron beam from penetrating through the walls to observe the image of prepared composites. The TEM images of wt% GO/MIL-101(Al) noticed a layered structure of the sheets of GO, which indicate that the GO sheet already loaded on the surfaces of MIL-101 crystals.

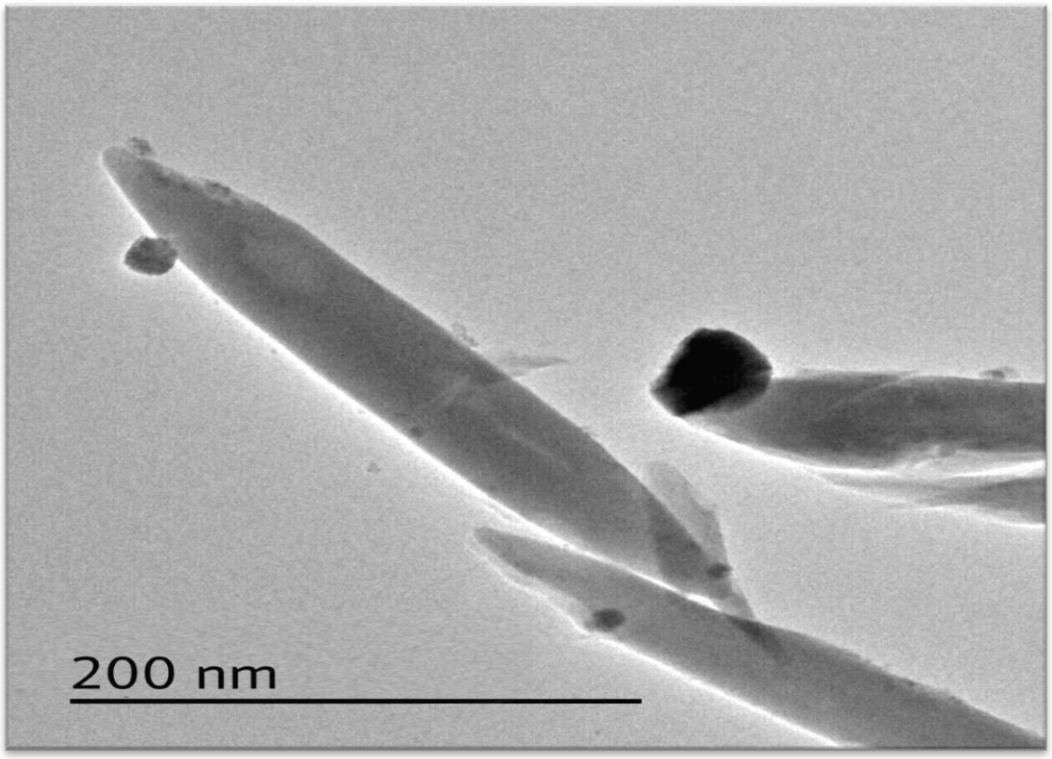

Fig 4a: TEM image MIL-101 (Al)

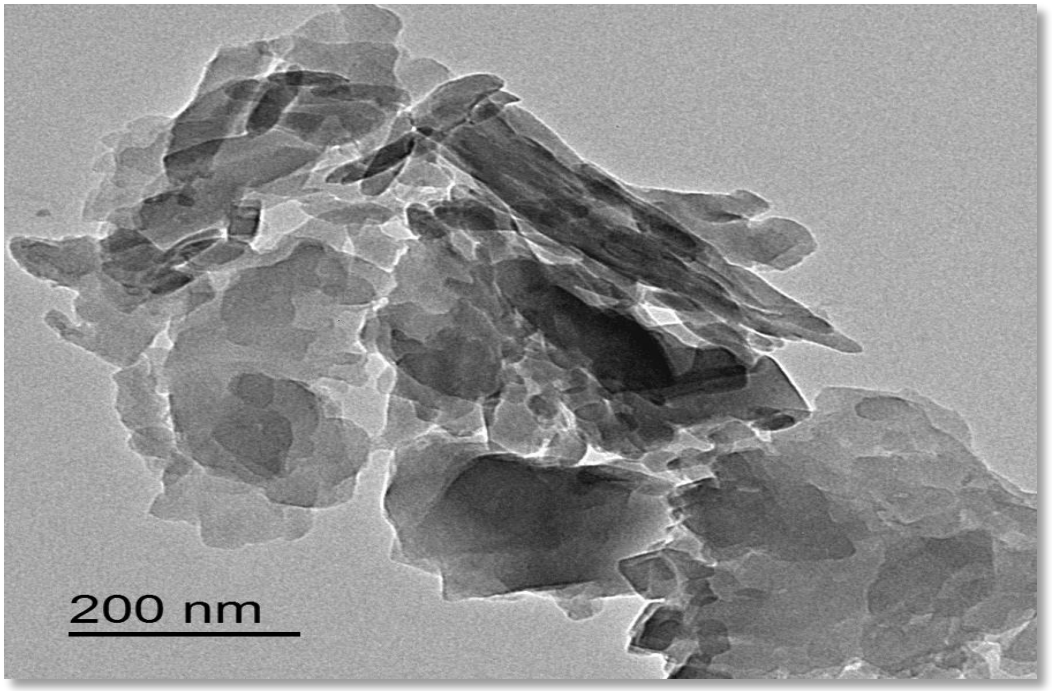

Fig. 4b: TEM image 1wt% GO/MIL-101 (Al)

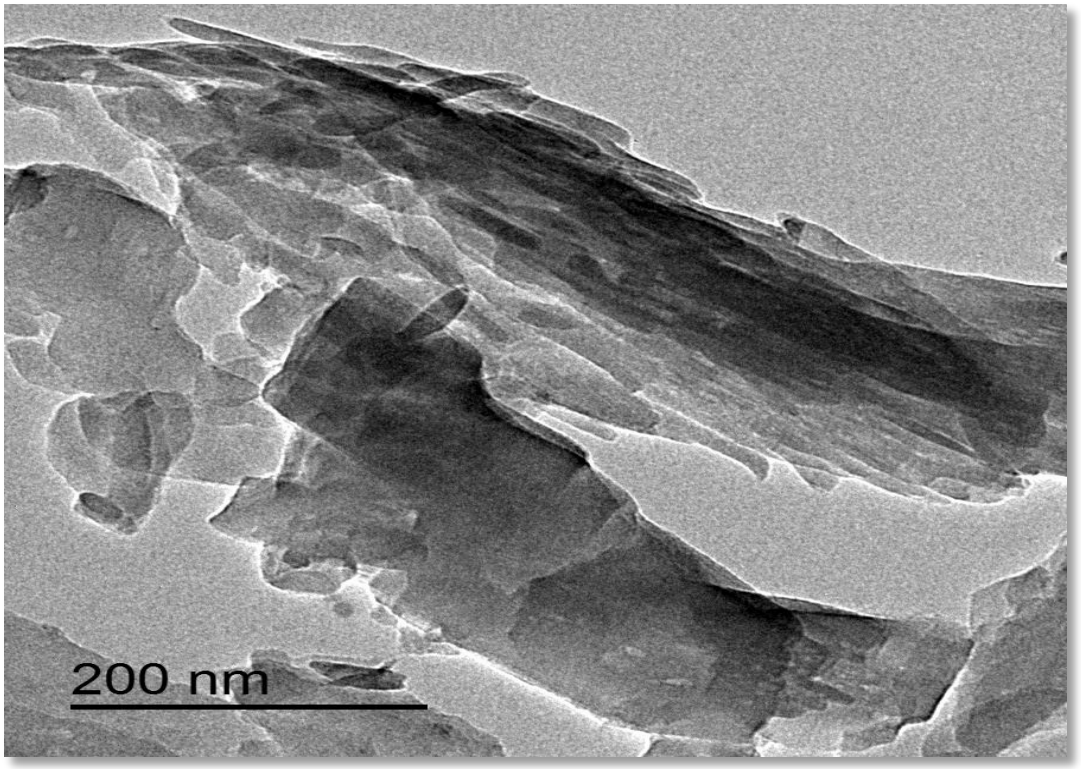

Fig. 4c: TEM image 5 wt% GO/MIL-101 (Al)

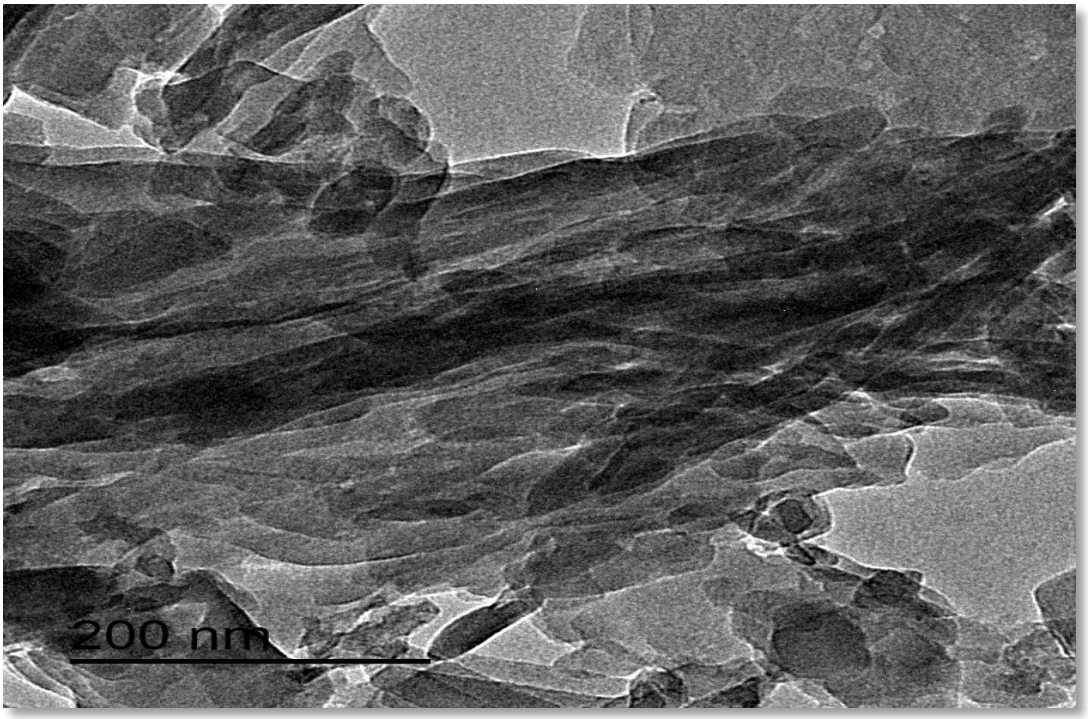

Fig. 4d: TEM image 10 wt% GO/MIL-101 (Al)

3.2. Adsorption

3.2.1. Effectiveness of contact time

The effectiveness of contact time on the process of adsorption of CR dye onto MIL-101 and different wt% GO/MIL-101 Al is plotted in Figure 5. The resulting data showed that the percentage of azodye removal declined by increasing contact time (The CR concentration 100 ppm and 0.03 weight of nanocatalysts). 1 wt% GO/MIL-101 Al sample rapidly absorbed up to 44% within 15 mins, while MIL-101 Al absorbed 22% of dye concentration. The percentage increased until reached equilibrium up to 96% within 120 mins for 1 wt% GO/MIL-101 Al, while equilibrium for MIL-101 Al reached 74% no more.

The large removal percentage at the start of the contact time was because of the high amount of pores available for adsorption process of the dye during the first stage [61]. After increasing time the number of pores available decrease so the removal rate decrease until equilibrium since the few remaining unoccupied spaces on surface sites became difficult to be activated because of expelling forces between the solute molecules on the solid and bulk phases. The percentage removal by 1 wt% GO/MIL-101 is larger than MIL-101 may be because of large in size of pores that affected also the kinetics of adsorption [62].

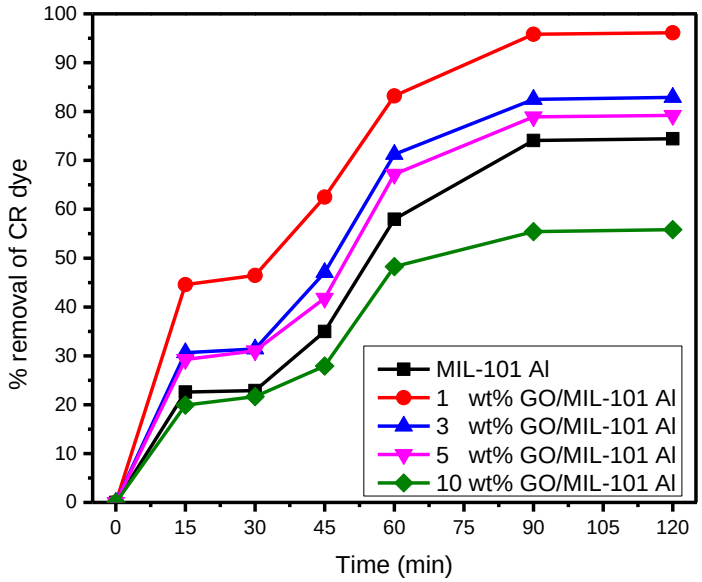

Fig. 5: Effectiveness of contact time on adsorption of CR on MIL-101 Al and different wt. % GO/MIL-101 Al in 2 hrs.

3.2.2. Effectiveness of Congo Red azodye concentration

The effectiveness of dye concentration as pollutants on adsorption of CR onto MIL-101 (Al) and different wt% GO/MIL-101 is shown in Fig. 6. Effect of initial concentration dye using 50, 100,150, 200, 250, 300 and 400 ppm of congo red dye solution was studied using a constant time of 2 hrs, weight 0.03 g catalyst and a temperature of 25 ^{o}C on MIL-101 (Al) and 1, 3, 5 and 10 wt% GO/MIL-101 samples. The results showed that the removal percentage decreased by increasing the dye concentration above 50 ppm.

The decline of the adsorption removal percentage with an increase in the initial CR dye concentration in solution may be because of the aggregation of CR dye molecules may be due to the competition of the molecules to enter inside the pores on the catalyst surface. Likewise, the decline of unoccupied activated adsorption sites in the surface area was a reason for the declining of removal percentage because the ratio between CR molecules to the catalyst weight increased with increasing of the initial dye concentration [63]. It could also be shown that the adsorption by MIL-101 was lower than that of 1, 3 and 5 wt% GO/MIL-101 nanocatalysts, but it was higher than that of 10%wt GO/MIL-101. The removal percentage of MIL-101 improved for CR from, 74.08% to 95.83%. This data indicated that loading GO on MIL-101 (Al) surface would help in improving the adsorption percentage while raising the percentage of GO will be counterproductive. So, the preferred percentage of GO in the GO/MIL-101 (Al) was 1wt% GO/MIL-101 (Al) [57].

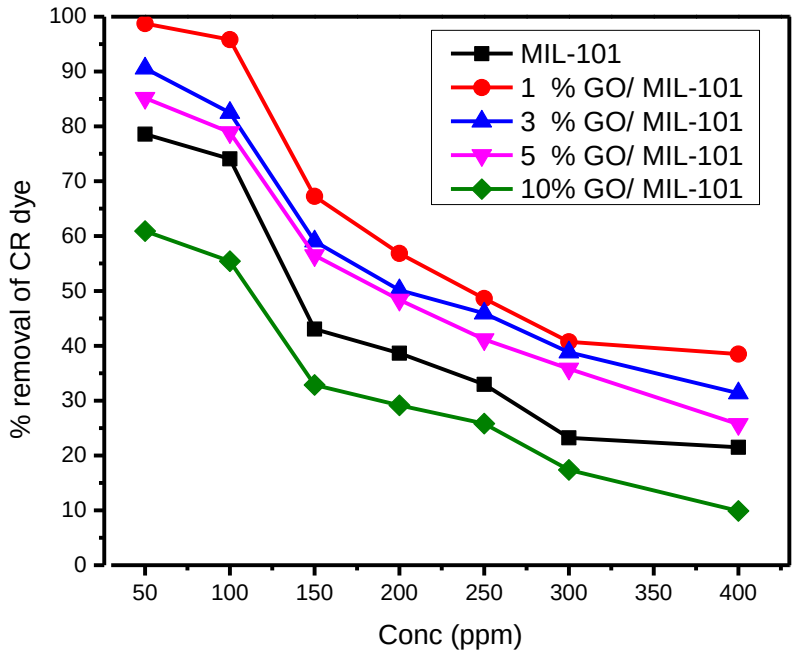

Fig. 6: Effectiveness of dye concentration on adsorption process of CR on MIL-101 and different wt % GO/MIL-101 in 2 hrs.

3.2.3. Effectiveness of catalyst weight

The effectiveness of catalyst weight on adsorption of CR onto MIL-101 and wt% GO/MIL-101 was noticed in Figure 7. The effect of catalyst dosage using weight 0.02, 0.03, 0.04, 0.05 and 0.06 g of prepared samples was studied using a constant time 2 hrs, concentration 100 ppm and a temperature of 25 ^{o}C on MIL-101 (Al) and 1, 3, 5 and 10wt.% GO/MIL-101 (Al). The resulting data indicating that removal of CR dye increased with an increase of catalysts weight for all prepared samples, because of the availability of more

surface area on a surface of the samples [64]. The results show that the removal percentage by MIL-101 (Al) was increased from 57% to 85% when catalyst dosage increased from 0.02 g to 0.06 g, while for 1 wt% GO/MIL-101 (Al) sample, the removal was increased from 81% to 98% when catalyst dosage increased from 0.02 g to 0.06 g.

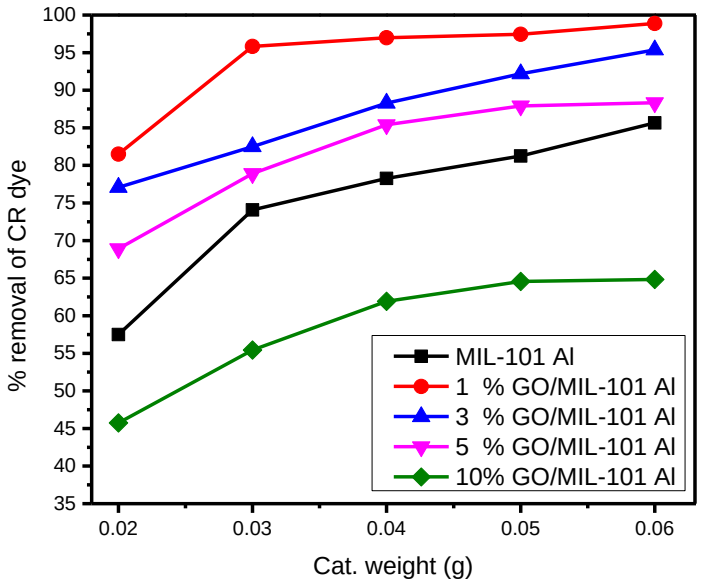

Fig. 7: Effectiveness of catalysts dosage on the adsorption process of CR on MIL-101 and different wt% GO/MIL-101 in 2 hrs.

3.2.4. Adsorption isotherms

A relationship between adsorption capacity of prepared nanocatalysts and dyes concentration can be expressed using the Langmuir and the Freundlich adsorption equations [55]. The equilibrium results for congo red dye over the concentration range from 50 to 400 mg/L 25°C were fit to the Langmuir model not the freundlish model. The data in Figs (8, 9, 10) give a linear form for Langmuir parameters. R^2 value for MIL Al was (0.9984) according to Langmuir model and (0.1525) according to Freundlich model, while R^2 value for 1 wt% GO/MIL-101 (Al) was (0.9990) according to Langmuir model and (0.8404) according to the Freundlich model (Table1). The R_L value was between 0 and 1 indicating that the adsorption of congo red dye was appropriate.

- Langmuir model can be written:

$$\frac{1}{\mathrm{qe}} = \frac{1}{\mathrm{Kqm}} + \frac{1}{\mathrm{ce}}$$

- The linear form of Langmuir isotherm can be represented as:

$$\frac{\mathrm{C}_e}{\mathrm{q}_e} = \frac{1}{R_L q_m} + \frac{\mathrm{C}_e}{q_m}$$

- Freundlich model can be written :

$$q_e = K_f C^{1/n}$$

- The linear form of Freundlich isotherm can be represented as:

$$In\ q_e = (1/n)\ In\ C_e + In\ K_f$$

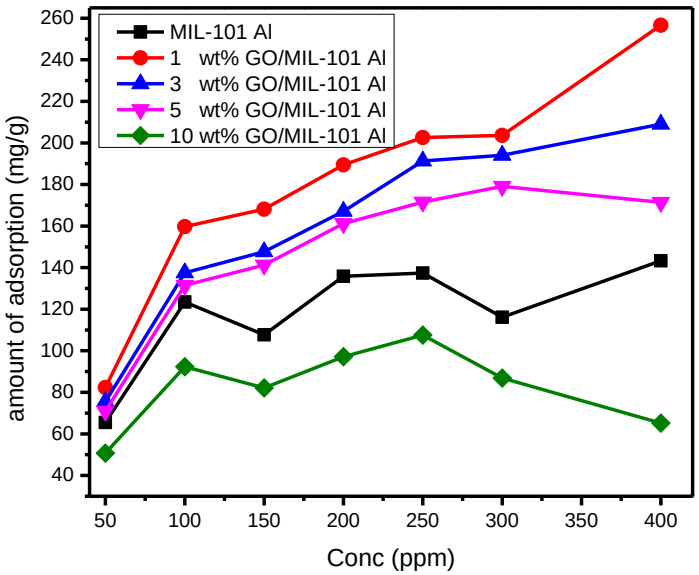

Fig. 8: Equilibrium adsorption isotherms for MIL-101 Al and different wt% GO/MIL-101 Al at concentrations from 50-400 mg/L

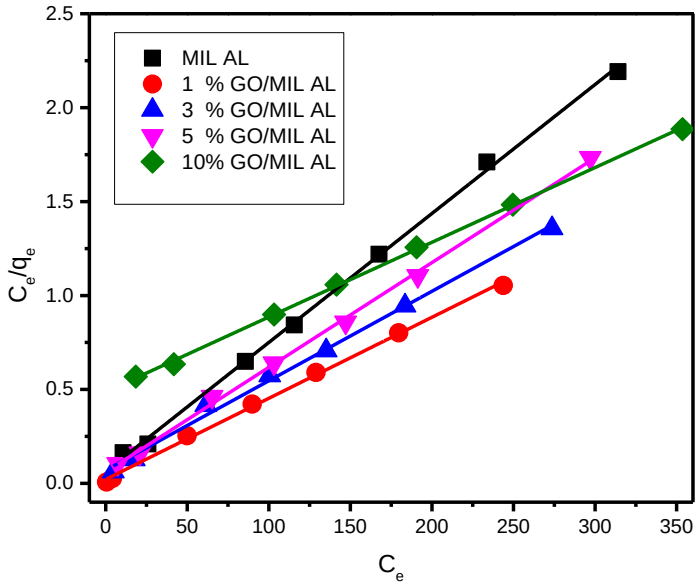

Fig. 9: The Linear form of Langmuir isotherm for CR on MIL-101 and wt% GO/MIL-101

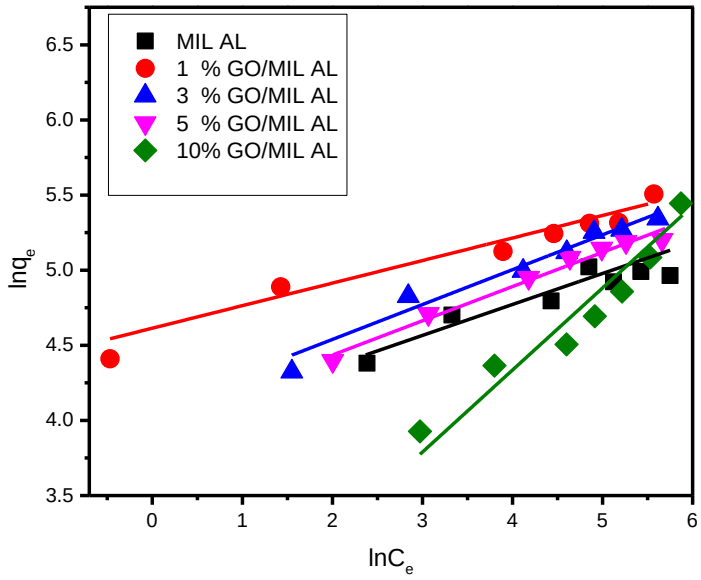

Fig. 10: The Linear form of Freundlich isotherm for CR on MIL-101 and wt% GO/MIL-101

Table 1: Adsorption isotherm parameters for Congo Red on MIL-101 and wt% GO/MIL-101.

samples	***Langmuir isotherm***				***Freundlich isotherm***		
	q_{max} ***(mg/g)***	k_L ***(L/mg)***	R^2	R_L	k_F ***(mg/g)***	***N***	R^2
MIL-101 Al	145.56	0.107	0.9984	0.022	51.80	4.85	0.1525
1 wt% GO/MIL	232.01	0.201	0.9990	0.012	100.87	6.66	0.8404
3 wt% GO/MIL	210.08	0.067	0.9948	0.035	58.83	4.30	0.9149
5 wt% GO/MIL	179.21	0.092	0.9981	0.026	53.500	4.38	0.8216
10 wt% GO/MIL	251.25	0.0081	0.9983	0.235	8.595	1.83	0.3644

3.2.5. Kinetic study

Dynamic adsorption is a major property when regarding the calculation of the amount of adsorption. The adsorption of pollutants from aqueous solutions by solid catalysts is an occurrence which usually involves complex kinetics. The rate of adsorption of pollutants is highly affected by a lot of parameters attached to the state of nanocatalysts as adsorbents, which has a heterogeneous surface in a lot of cases, and to the physical and chemical conditions under which adsorption has happened. We can express kinetic study using pseudo first-order kinetic study [65] and pseudo second-order kinetic study [66]. The followed equations expressed the two types.

- Pseudo- First - Order model:

$$\frac{\mathrm{dqt}}{\mathrm{dt}} = K_1 (q_e - q_t)$$

$$ln(q_e - q_t) = In\, q_e - K_1 t$$

- Pseudo - Second - Order model:

$$\frac{dqt}{dt} = K_2 (q_e - q_t)^2$$

$$\frac{\mathrm{t}}{q_t} = \frac{1}{K_2 q_{e2}} + \frac{1}{q_e}\,\mathrm{t}$$

The suitable curves resulting from the linearized-integral form of pseudo-first-order and pseudo-second-order for CR azodye are plotted in Figure 12 and 13, respectively. The kinetic parameter values for the studied models were determined and the results are given in (Table 2) along with the correlation coefficient. It can be noticed that pseudo - second order kinetic study gives a better correlation coefficient (R^2, near to 1) for the adsorption process of dyes on the samples. Also, the q_e value determined by the pseudo-second-order model, represents a good agreement with the calculated value in the experiment. Subsequently, the pseudo-second-order kinetic study is the best model for description correctly the kinetic action of CR dye by all adsorbents. It is also proposed an assumption behind the pseudo-second-order kinetic study, that the rate-limiting step of dyes uptake process is the results of chemisorption and more than one-step may be implicated in the sorption process [67, 68] .

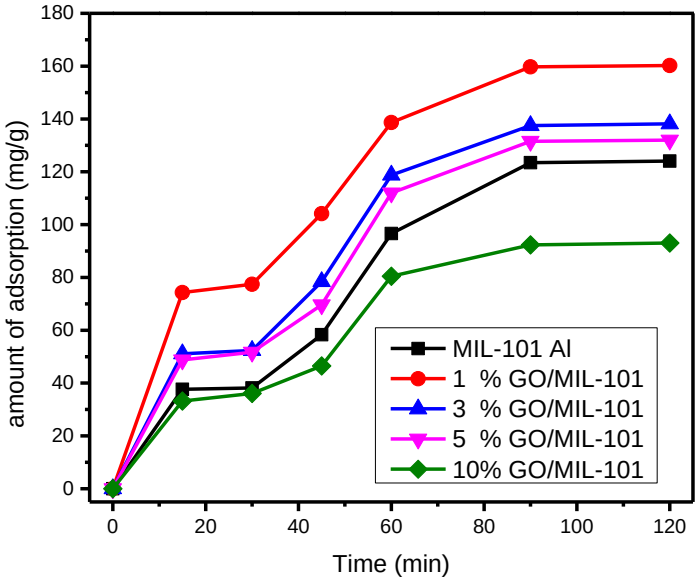

Fig. 11: Kinetic study of MIL-101 Al and wt% GO/MIL-101 Al

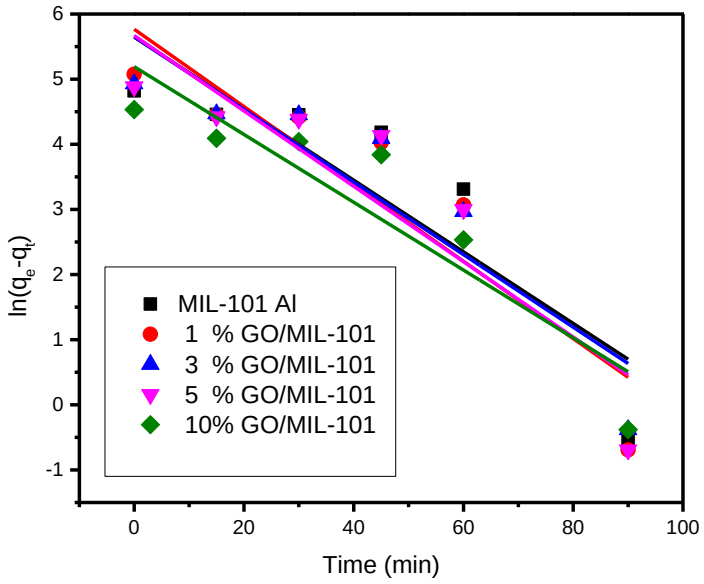

Fig. 12: Pseudo first-order kinetic study for adsorption of CR on MIL-101 and on wt% GO/MIL-101

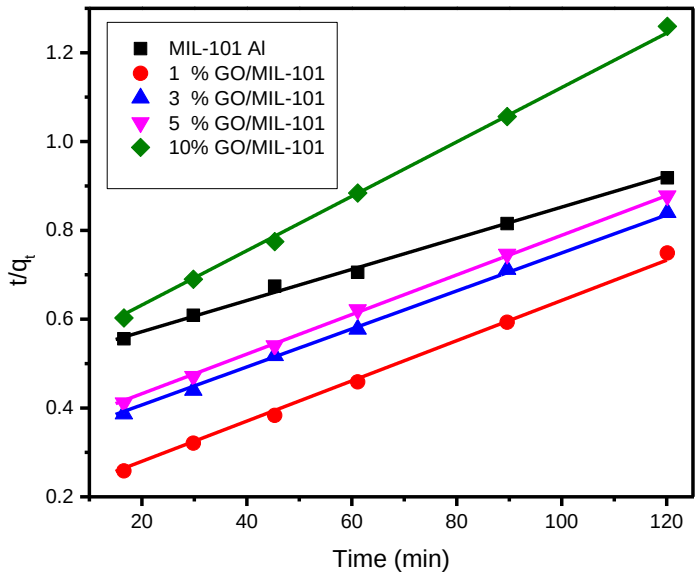

Fig. 13: Pseudo second order kinetic study for adsorption of CR on MIL-101 and wt% GO/MIL-101

Table 2: kinetic model parameters (pseudo 1st order and pseudo 2nd order) for adsorption process of Congo Red on MIL-101 and on wt% GO/MIL-101

samples	$q_{e(exp)}$ *(mg/g)*	*Pseudo first-order kinitic model*			*Pseudo second-order kinitic model*		
		q_{e1} *(mg/g)*	k_1 *(L/hr)*	R^2	q_{e2} *(mg/g)*	$k_2 * 10^{-3}$ *(g/mg.hr)*	R^2
MIL-101(Al)	123.46	0.89	4.67	0.9173	120.33	3.70	0.9845
1 wt% GO/MIL	156.71	0.902	4.62	0.9955	155.76	6.00	0.9971
3 wt% GO/MIL	137.5	0.907	4.55	0.9506	139.66	4.14	0.9897
5 wt% GO/MIL	131.51	0.917	4.57	0.9123	122.54	5.43	0.9928
10 wt% GO/MIL	92.35	0.942	4.16	0.9107	80.19	10.63	0.9968

4. Conclusion

In this paper, a novel wt%GO/MIL-101 (Al) composite nanocatalyst was prepared for the adsorption process for getting rid of Congo Red from the water. This nanocatalyst indicated improved adsorption activity compared to MIL-101 (Al), showing that the presence of GO played an important role in the adsorption activity. The pseudo-second-order kinetic and Langmuir isotherm adsorption models expressed well the adsorption of Congo Red dye on the nanocatalyst. All these results proposed that GO/MIL-101 (Al) may be a good adsorbent for the treatment of dyeing wastewater.

References

[1] Prasanth K.P., Rallapalli P., Manoj C. R., Bajaj H.C., Jasra R. V., Enhanced hydrogen sorption in single walled carbon nanotube incorporated MIL-101 composite metaleorganic framework, *Int. J. Hydrogen Energy*, 2011, 36: 7594-7601.

[2] Chae H. K., Siberio-Pe´rez D. Y., Kim J., Go Y., Eddaoudi M., Matzger A. J., O'Keeffe M., Yaghi O. M., A route to high surface area, porosity and inclusion of large molecules in crystals , *Nature*, 2004, 427: 523-527.

[3] Adeyemo A. A., Adeoye I. O., Bello O. S., Metal organic frameworks as adsorbents for dye adsorption: overview, prospects and future challenges, Toxicol. *Environ. Chem*., 2012, 94: 1846–1863.

[4] Rowsell J. L. C., Yaghi O. M., Metal–organic frameworks: a new class of porous materials, *Microporous Mesoporous Mater*., 2004, 73: 3-14.

[5] Natarajan, S., Mahata P., Metal-organic framework structures – how closely are they related to classical

inorganic structures? , *Chem. Soc. Rev*., 2009, 38: 2304.

[6] Long J. R., Yaghi O. M., The pervasive chemistry of metal-organic frameworks, *Chem. Soc. Rev*., 2009, 38: 1213-1214.

[7] Meek S. T., Greathouse J. A., Allendorf M. D., Metal-Organic Frameworks: A Rapidly Growing Class of Versatile Nanoporous Materials, *Adv. Mater*., 2011, 23: 249 -267.

[8] Assfour B, Seifert G., Hydrogen storage in 1D nanotube-like channels metal-organic frameworks: effects of free volume and heat of adsorption on hydrogen uptake. *Int. J. Hydrogen Energy*, 2009, 34: 8135-8143.

[9] Li J.R., Sculley J., Zhou H.C., Metal-organic frameworks for separations, *Chem. Rev.*, 2012, 112: 869-932.

[10] Zhu Q.L., Xu Q., Metal-organic framework composites, *Chem. Soc. Rev.*, 2014 43: 5468-5512.

[11] Lykourinou V., Chen Y., Wang X. S., Meng L., Hoang T., Ming L. J., Musselman R. L. , Ma S., Immobilization of MP-11 into a Mesoporous Metal-Organic Framework, MP-11@mesoMOF: A New Platform for Enzymatic Catalysis, *J. Am. Chem. Soc.*, 2011, 133: 10382-10385.

[12] Kreno L. E., Hupp J. T., Van Duyne R. P., Metal-organic Framework Thin Film for Enhanced Localized Surface Plasmon Resonance Gas Sensing, *Anal. Chem.*, 2010, 82: 8042-8046.

[13] Yang S. J., Choi J. Y., Chae H. K., Cho J. H., Nahm K. S., Park C. R., Preparation and Enhanced Hydrostability and Hydrogen Storage Capacity of CNT@MOF-5 Hybrid Composite, *Chem. Mater.*, 2009, 21: 1893-1897.

[14] Stankovich S., Dikin D.A., Dommett G.H., Kohlhaas K.M., Zimney E.J., Stach E.A., Piner R.D., Nguyen S.T., Ruoff R.S., Graphene-based composite materials, Nature , 2006, 442: 282-286.

[15] Compton O.C., Nguyen S.T., Graphene oxide, highly reduced graphene oxide, and graphene: versatile building blocks for carbon-based materials, *Small*, 2010, 6: 711-23.

[16] Liu S.B., Zeng T.H., Hofmann M., Burcombe E., Wei J., Jiang R.R., Kong J., Chen Y., Antibacterial activity of graphite, graphite oxide, graphene oxide, and reduced graphene oxide: membrane and oxidative stress, *ACS Nano* , 2011 5: 6971-6980.

[17] Park S., An J.H., Jung I.W., Piner R.D., An S.J., Li X.S., Velamakanni A., Ruoff R.S., Colloidal suspensions of highly reduced graphene oxide in a wide variety of organic solvents, Nano Lett., 2009, 9: 1593-1597.

[18] Crini G., Kinetic and equilibrium studies on the removal of cationic dyes from aqueous solution by adsorption onto a cyclodextrin polymer , *Dyes Pigm.*, 2008, 77: 415-426.

[19] Gong R., Ding Y., Li M., Yang C., Liu H., Sun Y., Utilization of powdered peanut hull as biosorbent for removal of anionic dyes from aqueous solution, *Dyes Pigm.*, 2005, 64: 187-192.

[20] Pokhrel D.,Viraraghavan T., Treatment of pulp and paper mill wastewatere a review, *Sci. Total Environ*., 2004, 333: 37-58.

[21] Anjaneyulu Y., Chary N. S., Raj D. S. S., Decolourization of industrial effluents-available methods and emerging technologies a review, *Rev. Environ Sci. Biotechnol*, 2005, 4: 245-273.

[22] Rai H. S., Bhattacharyya M.S., Singh J., Bansal T.K., Vats P., Banerjee U.C., Removal of dyes from the effluent of textile and dyestuff manufacturing industry: a review of emerging techniques with reference to biological treatment, *Crit. Rev. Environ. Sci. Technol.* , 2005, 35: 219-238.

[23] Crini G, Non-conventional low-cost adsorbents for dye removal, a review, *Bioresource Technology*, 2006, 97: 1061-1085.

[24] Vajnhandl S, Marechal A. M. L., Ultrasound in textile dyeing and the decolouration/mineralization of textile dyes, *Dyes Pigm*., 2005, 65: 89-101.

[25] Purkait M.K., Vijay S.S., DasGupta S., De S., Separation of congo red by surfactant mediated cloud point extraction , *Dyes Pigm*., 2004, 63: 151-159.

[26] Neamtu M., Yediler A., Siminiceanu I., Macoveanu M., Kellrup A., Decolorization of disperse red 354 azo dye in water by several oxidation processes a comparative study, *Dyes Pigm*., 2004, 60: 61-68.

[27] Chakraborty S., Purkait M.K., DasGupta S., De S., Basu J.K., Nanofiltration of textile plant effluent for color removal and reduction in COD, *Sep Purif Technol*, 2003, 31: 141-151.

[28] Zhang F., Yediler A., Liang X., Kettrup A., Effect of dye additives on the ozonation process and oxidation byproducts: a comparative study using hydrolyzed C.I. Reactive Red 120, *Dyes Pigm*., 2004, 60: 1-7.

[29] Aksu Z., Application of biosorption for the removal of organic pollutants, a review, Process Biochem., 2005, 40: 996-1026 .

[30] Dabrowski A. , Adsorption, from theory to practice, *Adv. Colloid Interface*, 2001, 93: 135-224.

[31] Jain A. K., Gupta V. K., Bhatnagar A., Suhas, Utilization of industrial waste products as adsorbents for the removal of dyes, *J. Hazard. Mater.* , 2003, B101: 31-42.

[32] Ozcan A. S., Ozcan A., Removal of Congo red using activated carbon and its regeneration, J. *Colloid Interface Sci.*, 2004, 276: 39-46.

[33] Lata H., Mor S., Garg V. K., Gupta P. K., Removal of a dye from simulated wastewater by adsorption using treated parthenium biomass , *J. Hazard. Mater.*, 2008, 153: 213–220.

[34] Arslan M., Rigitoglu M., Adsorption Behavior of Congo Red from an Aqueous Solution on 4-Vinyl Pyridine Grafted Poly(ethylene terephthalate) Fibers, *J. Appl. Polym. Sci.*, 2008, 107: 2846-2853.

[35] Sun Q., Yang L., The adsorption of basic dyes from aqueous solution on modified peat-resin particle, *Water Res.* , 2003, 37: 1535–1544.

[36] Haque E., Lo V., Minett A. I., Harris A. T., Church T. L., Dichotomous adsorption behaviour of dyes on an amino-functionalised metal-organic framework, amino-MIL-101(Al), *J. Mater. Chem*., 2014, 2: 193-203.

[37] Petit C., Bandosz T. J., MOF-graphite oxide nanocomposites: surface characterization and evaluation as adsorbents of ammonia, *J. Mater. Chem*., 2009, 19: 6521-6528.

[38] Bandosz T. J., Petit C., MOF/graphite oxide hybrid materials: exploring the new concept of adsorbents and catalysts, Adsorpt. *J. Int. Adsorpt. Soc*., 2011, 17: 5-16.

[39] Petit C., Bandosz T. J., Synthesis, characterization, and ammonia adsorption properties of mesoporous metal-organic framework (MIL(Fe))-Graphite oxide composites: exploring the limits of materials fabrication, Adv. Funct. Mater., 2011, 21: 2108-2117.

[40] Zhang Y., Li G., Lu H., Lv Q., Sun Z. G., Synthesis, characterization and photocatalytic properties of MIL-53(Fe)-graphene hybrid materials, *RSC Adv.* , 2014, 4: 7594-7600.

[41] Zhou X., Huang W.Y., Shi J., Zhao Z. X., Xia Q.B., Li Y. W., Wang H. H., Li Z., A novel MOF/graphene oxide composite GrO@MIL-101 with high adsorption capacity for acetone, *J. Mater. Chem*., 2014, A 2: 4722-4730.

[42] serra-crespo P., Ramos–Fernandez E. V., Gascon J., captain F., Synthesis and Characterization of an Amino Functionalized MIL-101(Al): Separation and Catalytic Properties, *Chem. Mater*., 2011, 23: 2565-2572.

[43] Kavitha M. K., Pillai S. C., Gopinath P., John H., Hydrothermal synthesis of ZnO decorated reduced graphene oxide: Understanding the mechanism of photocatalysis, *J. Environ. Chem. Eng*., 2015, 2: 1194-1199 .

[44] Kovtyukhova N. I., Ollivier P. J., Martin B. R., Mallouk T. E., Chizhik S. A., Buzaneva E.V., Gorchinskiy A. D., Layer-by-Layer Assembly of Ultrathin Composite Films from Micron-Sized Graphite Oxide Sheets and Polycations, *J. Mater. Chem*., 1999, 11: 771-778.

[45] Cao A., Liu Z., Chu S., Wu M., Ye Z., Cai Z., Chang Y., Wang S., Gong Q. , Liu Y., A Facile One-step Method to Produce Graphene–CdS Quantum Dot Nanocomposites as Promising Optoelectronic Materials, *Adv. Mater*., 2010, 22: 103-106.

[46] Guo S. , Dong S., Graphene nanosheet: synthesis, molecular engineering, thin film, hybrids, and energy and analytical applications, *Chem. Soc. Rev*., 2011, 40: 2644-2672.

[47] Rao C. N. R., Subrahmanyam K. S., RamakrishnaMatte H. S. S. , Maitra U., Moses K., Govindaraj A., Graphene: synthesis, functionalization and properties, *Int. J. Mod. Phys B*, 2011, 25: 4107-4143.

[48] Chatterjee S., Lee D. S., Lee M. W., Woo S. H., Enhanced adsorption of congo red from aqueous solutions by chitosan hydrogel beads impregnated with cetyl trimethyl ammonium bromide, *Bioresour.*

Technol., 2009, 100: 2803-2809.

[49] Wang L., Wang A., Adsorption properties of congo red from aqueous solution onto N,O-carboxymethyl-chitosan, *Bioresour. Technol.*, 2008, 99: 1403-1408.

[50] Chatterjee S., Lee M. W., Woo S. H., Influence of impregnation of chitosan beads with cetyl trimethyl ammonium bromide on their structure and adsorption of congo red from aqueous solutions, *Chem. Eng. J.*, 2009, 155: 254-259.

[51] Barthelet K., Marrot J., Ferey G., Riou D., V-III(OH){O_2C-C_6H_4-CO_2}(center dot)(HO_2C-C_6H_4-CO_2H)(x)(DMF)(y)(H_2O)(z)(or MIL-68), A new vanadocarboxylate with a large pore hybrid topology: reticular synthesis with infinite inorganic building blocks?, *Chem. Commun*., (2004) 520-521.

[52] Seoane B., Sebastian V., Tellez C., Coronas J., Crystallization in THF: the possibility of one-pot synthesis of mixed matrix membranes containing MOF MIL-68(Al), *Cryst. Eng. Comm*., 2013, 15: 9483-9490.

[53] Petit C., Burress J., Bandosz T. J., The synthesis and characterization of copper based metal-organic framework/graphite oxide composites, *Carbon*, 2011, 49: 563-572.

[54] Cai D.Y., Song M., Preparation of fully exfoliated graphite oxide nanoplatelets in organic solvents, *J. Mater. Chem.*, 2007, 17: 3678-3680.

[55] Yang C., Wu S., Cheng J., Chen Y., Indium-based metal-organic framework/ graphite oxide composite as an efficient adsorbent in the adsorption of rhodamine B from aqueous solution, *J. Alloys Compd.* ,2016, 687: 804-812.

[56] Zhang Y., Li G., Lu H., Lv Q., Sun Z.G., Synthesis, characterization and photocatalytic properties of MIL-53(Fe)-graphene hybrid materials, *RSC Adv.* , 2014, 4: 7594-7600.

[57] Wu S., Yu L. , Xiao F. , You X., Yang C. , Cheng J. ,Synthesis of aluminum-based MOF/graphite oxide composite and enhanced removal of methyl orange, *J Alloys Compd* , 2017, 724: 625-632.

[58] Szabó T., Berkesi O., Dékány I., DRIFT study of deuterium-exchanged graphite oxide, *Carbon*, 2005, 43: 3186-3189.

[59] Pan D., Wang S., Zhao B., Wu M., Zhang H., Wang Y., Jiao Z., Li Storage Properties of Disordered Graphene Nanosheets , *Chem. Mater.* , 2009, 21: 3136-3142.

[60] Volkringer C., Loiseau T., Guillou N., Ferey G., Elkaïm E., Vimont A., XRD and IR structural investigations of a particular breathing effect in the MOF-type gallium terephthalate MIL-53(Ga), *Dalton Trans*. , 2009 , 2241- 2249.

[61] Chanzu H. A., Onyari J. M., shiunda P. M., Biosorption of malachite green from aqueous solutions onto polylactide/spent brewery grains films: kinetic and equilibrium studies, *J. Polym. Environ*., 2012, 20: 665-672.

[62] Hobday M. D., Li P. H. Y., Crewdson D. M., Bhargava S. K., The use of low rank coal-based adsorbents for the removal of nitrophenol from aqueous solution , *Fuel*, 1994, 73: 1848-1854.

[63] Qaid F. A., Azzahari A. D., Yahaya A. H., Yahya R., Methylene blue removal from aqueous solution by adsorption using Jatropha seed husks-activated carbon activated with KOH, *Desalination Water Treat.*, 2016, 57: 246-253.

[64] Cui S., Zhang H. , Zhang L., Adsorption of methylene blue from aqueous solution using honeycomb-cinder, *Adv. Mat. Res*., 2012, 550: 2259-2262.

[65] Hwang K., Lee J., Shim W., Jang H. D., Lee S., Yoo S., Adsorption and photocatalysis of nanocrystalline TiO2 particles prepared by sol–gel method for methylene blue degradation, *Adv. Powder Techn.*, 2012, 23: 414.

[66] Srivastava V.C., Mall I. D., Mishra I. M., Adsorption of toxic metal ions onto activated carbon study of sorption behaviour through characterization and kinetics, *Chem. Eng. Process*, 2008, 47: 1269-1280.

[67] Zhou L., Wang Y., Liu Z., Huang Q., Characteristics of equilibrium, kinetics studies for adsorption of Hg(II), Cu(II), and Ni(II) ions by thiourea-modified magnetic chitosan microspheres, *J. Hazard. Mater.*, 2009, 161: 995-1002.

[68] Elass K., Laachach A., Alaoui A., Azzi M., Removal of methyl violet from aqueous solution using a stevensite-rich clay from Morocco, *Appl. Clay Sci.*, 2011, 54: 90.